Inorganic Chemistry

Article

pubs.acs.org/IC

Looking for New Hybrid Polymer Fillers: Synthesis of Nanosized α-Type Zr(IV) Organophosphonates through an Unconventional Topotactic Anion Exchange Reaction

Monica Pica,*[,†] Anna Donnadio,[†] Elisabetta Troni,[†] Donatella Capitani,[‡] and Mario Casciola[†]

[†]Department of Chemistry, Perugia University, Via Elce di Sotto 8, 06123 Perugia, Italy

[‡]Laboratorio di Risonanza Magnetica "Annalaura Segre", Istituto di Metodologie Chimiche, CNR, Via Salaria km 29.300, 00016 Monterotondo Scalo (RM), Italy

ABSTRACT: Gels of α-type zirconium(IV) phosphate alkylphosphonates, $ZP(C_n)_x$, were prepared by reacting, at room temperature, propanol intercalated nanosized α-zirconium phosphate (α-ZrP) with propanol solutions of alkylphosphonic acids (H_2C_n, n = number of carbon atoms in the alkyl chain = 4, 5, 6), with (H_2C_n/Zr) molar ratios in the range 0.4−4.0. ^{31}P MAS NMR showed the presence of resonances due to the phosphate and phosphonate groups bonded to the Zr atoms mainly by three oxygen atoms, as in the α-type layer. The composition of the $ZP(C_n)_x$ materials, obtained by thermogravimetric analysis, ranges from $x \approx 0.2$ to $x \approx 1.1$. On the basis of the NMR data and of the analysis of the X-ray patterns of gels and powders, it is inferred that the $ZP(C_n)_x$ compounds have an α-type layered structure and that the reaction between α-ZrP and H_2C_n is a topotactic anion exchange process. The evolution of the X-ray patterns during propanol deintercalation is consistent with a random distribution of the alkylphosphonate groups on the α-type layers which gives rise to porous pathways in the interlayer region. To test the possibility of using $ZP(C_n)_x$ as mechanical reinforcement of a polymer matrix, a starch membrane filled with 5 wt % $ZP(C_6)_{0.54}$ was prepared and characterized by stress−strain mechanical tests. Besides an excellent flexibility, this membrane exhibited a proportional increase of the Young's modulus by 230% in comparison with neat starch.

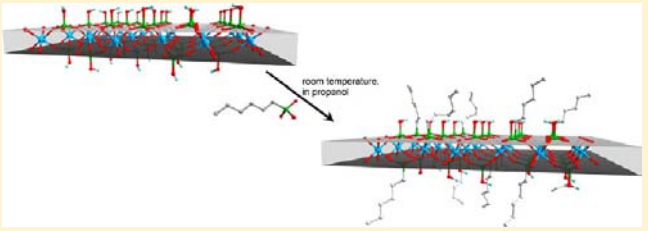

1. INTRODUCTION

The modification of inorganic materials by linking organic functional groups is a well-known and established strategy which has allowed to develop highly versatile materials by combining the robustness of the inorganic backbone with the reactivity due to the presence of the organic moiety.[1,2] An almost infinite range of inorgano−organo materials can be synthesized with a wide range of possible applications. As well as organically modified oxides,[1,2] surface modified metal phosphates,[2,3] and metal organo-phosphonates,[2,4] especially layered zirconium salts, were widely studied and explored as functional materials. Since 1978, when the first metal(IV) phosphonate with a layered structure was prepared,[5] much progress has been made in the synthesis of this class of materials and in their application as solid state proton conductors,[6] polymer fillers,[7] photochemical devices,[8] probes of DNA−protein interactions,[9] catalysts,[10] among many others.

As far as the synthetic approaches are concerned, zirconium-(IV) phosphonates can be prepared according to two main procedures:

(1) Direct synthesis, consisting in the reaction of Zr(IV) complexes with phosphonic acids or mixtures of phosphoric/phosphonic acid; this procedure is mainly used to obtain zirconium phosphonates with an α-type inorganic framework, $Zr(O_3PR)_2$;[4,7c−g,11]

(2) Topotactic exchange reaction, mainly used to prepare organic derivatives of γ-type zirconium phosphate ($ZrPO_4H_2PO_4{\cdot}2H_2O$, γ-ZrP). This procedure consists in the replacement of the $O_2P(OH)_2$ groups of γ-ZrP with organophosphonate groups, O_2PRR', by contacting microcrystals of the inorganic compound with a solution of the suitable phosphonic acid.[12] The reaction leaves the layer structure practically unchanged, and the phosphonate groups only affect the interlayer region.

While there are many examples in the literature on the topotactic exchange reactions involving γ-ZrP, only one paper reports the topotactic synthesis of α-type zirconium phosphonates from α-zirconium phosphate ($Zr(HPO_4)_2{\cdot}H_2O$, α-$ZrP{\cdot}H_2O$), in severe conditions of temperature and pressure and in the presence of the molten phosphonic acid.[13]

Recently, a new synthetic route has been developed for the synthesis of gels of α-ZrP nanocrystals, made of alcohol intercalated nanoplatelets.[14] These gels turned out to be very useful in the preparation of polymer nanocomposites, since the α-ZrP nanoplatelets are able to easily disperse within a polymer solution. Moreover, very preliminary results seem to prove that these nanoparticles could be employed also as catalyst supports, improving, at the same time, the catalyst activity. The high

Received: April 5, 2013
Published: June 13, 2013

dx.doi.org/10.1021/ic400834d | Inorg. Chem. 2013, 52, 7680−7687

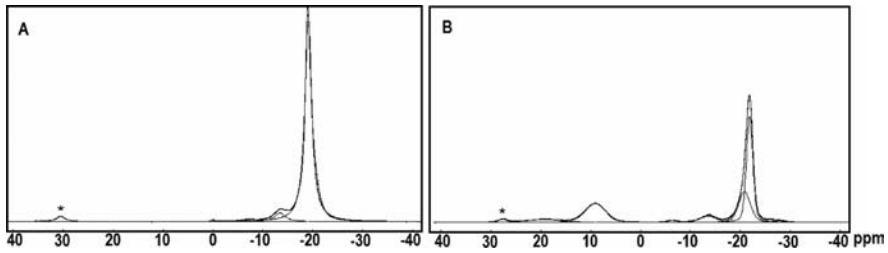

Figure 1. ^{31}P MAS NMR of pristine α-ZrP (A) and ZP$(C_6)_x$ obtained for R = 1.0 (B); the resonance labeled with an asterisk is a spinning sideband.

versatility of these materials stimulated our curiosity and drove us to investigate the reactivity of nanosized α-ZrP in topotactic exchange reactions. With this aim gels of α-ZrP nanoparticles in propanol were put in contact with solutions of alkylphosphonic acids at room temperature. Alkylphosphonic acids with different alkyl chain lengths were employed for the synthesis of the organo-derivatives of α-ZrP, as well as different (phosphonic acid/Zr) molar ratios. The synthesis successfully produced gels of propanol intercalated zirconium phosphate alkylphosphonates which were characterized, in terms of composition, particle morphology, and structure by thermogravimetric analysis, liquid and solid state ^{31}P NMR, X-ray diffraction, and scanning electron microscopy analysis. Moreover, the possibility to use these gels as source of nanoparticles for the preparation of polymer composites based on potato starch has been evaluated. A preliminary structural and mechanical characterization of a starch/zirconium phosphonate composite membrane was also reported.

2. EXPERIMENTAL SECTION

2.1. Chemicals. Alkylphosphonic acids ($H_2O_3PC_nH_{2n+1}$, hereafter H_2C_n, where n = 4, 6, 10) were purchased by Alfa Aesar. Zirconyl propionate ($ZrO_{1.27}(C_2H_5COO)_{1.46}$, MW = 218 Da) was supplied by MEL Chemicals, England. Native potato starch (amylose about 20%, amylopectin about 80%,) was kindly supplied by Novamont. All other reagents were supplied by Aldrich.

2.2. Synthesis of the Zirconium Alkylphosphonates. Zirconium alkylphosphonates were prepared by topotactic exchange reaction carried out on gels of nanosized α-ZrP in propanol, which were prepared according to ref 14. Specifically, 3.3 mmol of zirconyl propionate were dissolved in 10 mL of anhydrous propanol. Concentrated phosphoric acid was added, at room temperature under stirring, to the above solution so that the H_3PO_4/Zr molar ratio was 6. The clear solution obtained just after mixing turned into a semitransparent gel in few minutes. The gel, after washing with propanol, contained about 8 wt % α-ZrP.

Phosphonic acids, H_2C_n, were dissolved in propanol, so that the $[H_2C_n]$ was 0.1 M. A suitable volume of the H_2C_n solution was added to the ZrP gel in propanol, so that the (H_2C_n/Zr) molar ratio (hereafter referred to as R) was 0.4, 1.0, 2.0, 4.0. The mixture was kept stirring at room temperature for 3 days; then it was centrifuged obtaining a gelatinous compound, which was washed three times with propanol. The weight percent of the gels, determined by heating to dryness the wet samples, was in the range 8−11 wt %. The washed gel was dried in an oven at 60 °C, then washed in 10^{-3} M HCl, and dried again in an oven at 120 °C. All the zirconium alkylphosphonates will be hereafter indicated as ZP$(C_n)_x$.

2.3. Preparation of the Potato Starch Membrane Containing 5 wt % ZP$(C_6)_{0.54}$. One gram of native potato starch was dispersed in 25 mL of water and heated at 90 °C for 10 min until gelatinization occurred. A weighed amount of the ZP$(C_6)_{0.54}$ gel in propanol was first washed two times with water and then added to the cooled starch gelatin, and the mixture was left under stirring for 20 min at room temperature. The final dispersion was cast on a polystyrene dish and left in an oven at 40 °C overnight.

By using the same kind of procedure a starch film and starch/glycerol film containing 20 wt % glycerol were prepared. The films were 95−105 μm thick.

2.4. Techniques. X-ray diffraction patterns of gels, powders, and cast films were collected with a Philips X'Pert PRO MPD diffractometer operating at 40 kV and 40 mA, with a step size of 0.0334° and a scan step of 40 s, using Cu Kα radiation and an X'Celerator detector.

Thermogravimetric determinations were carried out by a NETZSCH STA 449 Jupiter thermal analyzer connected to a NETZSCH TASC 414/3 A controller at a heating rate of 10 °C/min, with an air flow of about 30 mL/min. Before measurements, all samples were equilibrated at 53% R.H.

Liquid ^{31}P NMR analysis was carried out by a Bruker advance DPX 400 MHz on solutions obtained by dissolving the solid samples (≈30 mg) in 3 M HF (≈2 mL). The shifts of the phosphoric and phosphonic acid signals, relative to 85% D_3PO_4 in D_2O, were +0.7 and +31 ppm, respectively.

Transmission electron microscopy (TEM) analysis was carried out by a Philips 208 transmission electron microscope, operating at an accelerating voltage of 100 kV. Powders were rapidly diluted in ethanol and sonicated for few minutes, then supported on copper grids (200 mesh) precoated with Formvar carbon films, and quickly dried.

Scanning electron microscopy (SEM) images of the membranes were collected by a Zeiss LEO 1525 FE SEM. The composite films were fractured in liquid N_2 and coated with a thin layer of chromium before SEM observation.

Solid state ^{31}P MAS NMR spectra were performed at 161.97 MHz on a Bruker Avance400 spectrometer. The powders were packed into 4 mm zirconia rotors and sealed with Kel-F caps. The spin rate was 8 kHz. The $\pi/2$ pulse width was 3.5 s, and the recycle delay was 140 s; 1200 scans were collected for each spectrum. Spectra of powdered samples were acquired using 2048 data points. All spectra were zero filled and Fourier transformed. The chemical shift was externally referred to H_3PO_4 85%. The deconvolution of ^{31}P MAS spectra was performed using the DM2006 program.[15] The Gaussian/Lorentzian model was selected. Each resonance was characterized by the amplitude, the resonance frequency in parts per million (ppm), and the width at half-height.

Stress−strain mechanical tests were carried out by a Zwick Roell Z1.0 testing machine, with a 200 N static load cell. Young's modulus (slope of stress−strain curve at low values of strain), yield stress (maximum stress that can be developed without causing plastic deformation) and elongation at break (ratio of elongation to original length of sample at break) were measured on rectangle shaped film stripes, obtained by a cutting machine, the length and width of which were 100 and 5 mm, respectively. Before testing, samples were equilibrated for 7 days in vacuum desiccators at R.H. of 33% and room temperature (20−23 °C), and the thickness of the film stripe, determined with an uncertainty of ±5 μm, was in the range 95−105 μm. An initial grip separation of 10.000 ± 0.002 mm and a crosshead speed of 5 mm/min was used. All tests were carried out at room temperature (20−23 °C). At least five replicate film stripes were analyzed. The data were elaborated by the TestXpert V11.0 Master software.

An ICP Varian Liberty inductively coupled plasma-optical emission spectrometry (ICP-OES) with axial injection was used for the quantitative analysis of zirconium and phosphorus. The samples to

dx.doi.org/10.1021/ic400834d | Inorg. Chem. 2013, 52, 7680−7687

be analyzed, dried overnight in an oven at 120 °C, were weighed and dissolved in 3 M HF (≈ 2 mL), and diluted with water.

3. RESULTS AND DISCUSSION

3.1. Material Characterization. *3.1.1. ^{31}P MAS NMR Characterization.* To get information about the occurrence of the reaction between H_2C_n and the α-ZrP gels, the solids were dried and studied by ^{31}P MAS NMR. The NMR spectrum of the pristine α-ZrP powder, reported in Figure 1A, shows the presence of one main signal at −19.1 ppm which is characteristic of monohydrogen phosphate group bonded to three Zr(IV) atoms in the α-layer,[16] while the weak signals at −13.4 and −7.9 ppm can be assigned to H_2PO_4 groups bonded to Zr(IV) through two and one oxygen atoms, respectively.[14]

Moreover, the sample shows also the presence of a very weak signal at +0.21 ppm, which is due to a negligible fraction of free phosphoric acid. Figure 1B shows the NMR spectrum of $ZP(C_6)_x$ obtained for R = 1.0. Similar spectra were obtained for all the $ZP(C_n)_x$ samples. In addition to the phosphate signals, other two resonances at +9.1 and +19.22 ppm are observed. Taking into account that the signal of free H_2C_6 lies at around +31 ppm, it is reasonable to attribute those resonances to the C_6 alkylphosphonate groups bonded to the Zr atoms through a different number of oxygen atoms, thus proving that the reaction between α-ZrP and H_2C_n effectively occurred.

In particular, since the phosphorus resonance shifts from 0 ppm for free phosphoric acid to around −19/−22 ppm when the phosphate group is bonded to three Zr atoms,[17] one can suppose a similar shift for the resonance of the phosphonate group, so that it passes from around +31 to +9.1 ppm when the three oxygen atoms of the phosphonic acid are connected to three Zr atoms. Similarly, the weak signal at +19.22 ppm can be assigned to HC_6 bonded to two Zr(IV) atoms. Notwithstanding the reaction occurred between α-ZrP and H_2C_n, it is also noteworthy that semitransparent gels, similar to the pristine material, were obtained and flocculation was not observed.

As far as the HPO_4 main resonance of Figure 1B is concerned, it was deconvoluted in two signals which are shifted to slightly more negative δ values with respect to that of pristine α-ZrP powder sample, lying at −21.9 and −20.9 ppm: similar values were found for the HPO_4 groups of the α-ZrP gel particles. In a previous work[14] it was inferred that during the drying process of the α-ZrP gel, nanocrystals may fuse together and increase their size, thus leading to a shift of the signal of the HPO_4 group in the ^{31}P MAS toward less negative δ values. As a consequence, one should conclude that when the α-ZrP gel particles react with H_2C_n, the particle growth, expected after solvent elimination, is hindered to some extent by the presence of the alkyphosphonate.

On the basis of the ^{31}P MAS NMR spectra, and taking into account that the (P/Zr) molar ratio of all materials is around 2, the following general formula for $ZP(C_n)_x$ can be written

$$Zr(OH)_{x'+y'}[O_2(OH)PC_nH_{2n+1}]_{x'}(O_3PC_nH_{2n+1})_{x''}$$
$$[O_2P(OH)_2]_{y'}(O_3POH)_{y''}$$

Putting $x' + x'' = x$, $y' + y'' = y$, and $x + y = 2$, the formula can be simplified as follows

$$Zr(O_3PC_nH_{2n+1})_x(O_3POH)_{2-x}\cdot(x' + y')H_2O$$

3.1.2. Composition. All the $ZP(C_n)_x$ samples were conditioned at 53% relative humidity and characterized by thermogravimetric (TG) analysis. As an example, Figures 2 and 3 report the TG curves of the $ZP(C_n)_x$ powder samples, obtained for R = 0.4 and 4.0.

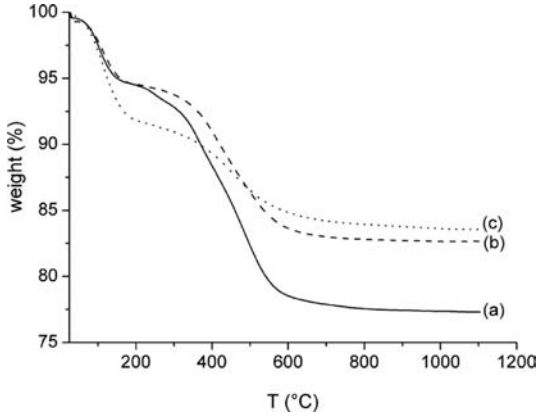

Figure 2. Thermogravimetric curves of $ZP(C_{10})_x$ (a), $ZP(C_6)_x$ (b), $ZP(C_4)_x$ (c) powder samples obtained for R = 0.4.

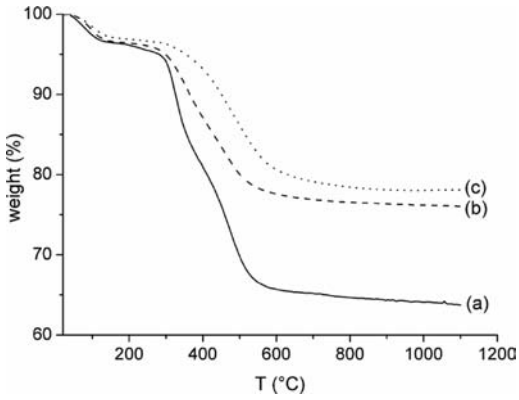

Figure 3. Thermogravimetric curves of $ZP(C_{10})_x$ (a), $ZP(C_6)_x$ (b), $ZP(C_4)_x$ (c) powder samples obtained for R = 4.0.

All materials exhibit weight losses larger than that of monohydrated α-ZrP (about 12 wt %): this is consistent with the presence of alkylphosphonate groups, in agreement with the ^{31}P MAS NMR data. The thermal decomposition of all solids takes place in two main steps; the first step, centered around 100 °C can be attributed to the loss of adsorbed and/or intercalated molecules, such as water and/or residual propanol. The second step, centered around 450−500 °C, can be mainly attributed to the decomposition of the hydrocarbon chains and to the loss of water arising from the condensation of residual HPO_4 groups. It is known that heating zirconium phosphonates in the presence of oxygen or air to temperatures between 1000 and 1200 °C leads to the formation of cubic zirconium pyrophosphate, ZrP_2O_7.[11b]

On the basis of these considerations, the weight loss corresponding to the second step of the thermogravimetric curve was used to determine the $ZP(C_n)_x$ composition. Table 1 reports the x value of the $ZP(C_n)_x$ samples, as function of R.

The x values determined by TG analysis agree, within 5%, with those found by liquid ^{31}P NMR analysis. To better highlight the relationship between the final composition of the materials and the initial amount of C_n within the reaction solution, the reaction percentage for the $ZP(C_n)_x$ samples was calculated from the ratio between x and 2, which is the total

dx.doi.org/10.1021/ic400834d | Inorg. Chem. 2013, 52, 7680−7687

Table 1. Chemical Composition of Zirconium Phosphate Alkylphosphonates, $ZP(C_n)_x$, Calculated from TG Analysis

	x			
n	R = 0.4	R = 1.0	R = 2.0	R = 4.0
4	0.19 ± 0.01	0.56 ± 0.03	1.07 ± 0.06	1.14 ± 0.07
6	0.30 ± 0.02	0.54 ± 0.03	0.80 ± 0.05	0.87 ± 0.05
10	0.34 ± 0.02	0.48 ± 0.03	0.96 ± 0.06	1.01 ± 0.06

number of reactive phosphate groups per Zr atom, according to the formula

$$\text{reaction\%} = \frac{x}{2}\cdot 100$$

Figure 4 displays the reaction percentage for the $ZP(C_n)_x$ samples as a function of R (solid lines): these values are

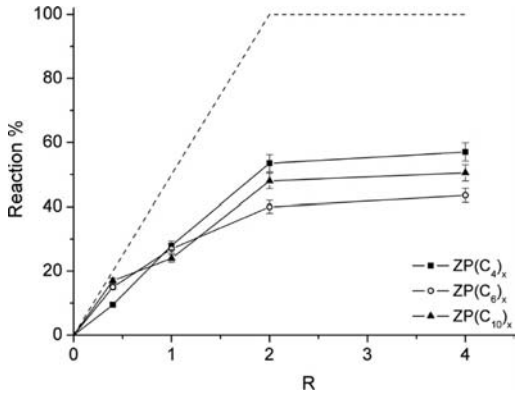

Figure 4. Reaction percentage values of $ZP(C_n)_x$ samples as function of R. The dashed line represents the achievable upper limit values.

compared with those representing the upper limit values (dashed line) calculated by assuming that, for $R \leq 2$, the phosphonic acid in solution completely reacts with ZrP (i.e., x = R), while for R = 4 the maximum amount of phosphonic acid cannot exceed the number of reactive phosphates (i.e., x = 2).

As a general trend, the experimental values of the reaction percentage lie below the achievable upper limit and become independent of R for $R \geq 2.0$, being around 50%. In particular, the reaction percentage (a) significantly increases when passing from C_4 to C_6 to C_{10} for R = 0.4, (b) shows similar values for R = 1, while (c) it slightly increases when passing from C_6 to C_{10} to C_4 for R > 1.

The observed trend is hard to explain, since several factors are involved in the reactions examined in this work. On one hand it should be considered that the reactions involving solids generally begin in the external part of the crystals[12c] and then proceed toward the internal part. The pristine material consists of propanol intercalated α-ZrP nanosheets, and it is believable that initially the phosphonic acids can easily diffuse within the layers and react. As the reaction proceeds, the reacted phase will result enriched in phosphonate groups, and, especially at high R values, the protruding phosphonate groups are expected to hamper the diffusion of additional phosphonic acid molecules within the interlayer space and their reaction with Zr(IV).

On the other hand the solvation of the phosphonic acid by propanol could affect its ability to react with Zr(IV). In this regard, D'Andrea et al.[18] found that the solvation of alkylphosphonic acids and their reactivity toward calcium hydroxyapatite range in opposite order. They explained the observed trends in terms of solvent−solute and solute-substrate interactions. When strong solvent−solute interactions were favored, the solute adsorption and reaction with the substrate diminished. However, in the case of weaker solvent−solute interactions, the solute-substrate interactions were more favored. In the present case, it is reasonable to suppose that the solvation energy of H_2C_n in propanol decreases with increasing the alkyl chain length because of an increasing difference in the polarity of the solvent and the solute. As a consequence, H_2C_{10} is expected to be less solvated and more reactive in propanol than H_2C_4. Therefore, it is reasonable to suppose that while the steric factors should promote the reaction of ZrP with H_2C_4 at high R values, the reduced solvation energy should favor the reaction of H_2C_{10} at low R values.

3.1.3. SEM Analysis. Figure 5a and 5b show the TEM images of the pristine α-ZrP and $ZP(C_{10})_{1.01}$ powder samples, respectively. It can be observed that while the starting material consists of layered particles with hexagonal shape and planar size in the range 50−300 nm, the zirconium phosphonate sample appears made of aggregates with an irregular shape, consisting of particles with size of some tens of nanometers and, on the whole, smaller than that of the unmodified α-ZrP. This observation is in agreement with what was supposed by NMR analysis, according to which when the α-ZrP gel particles

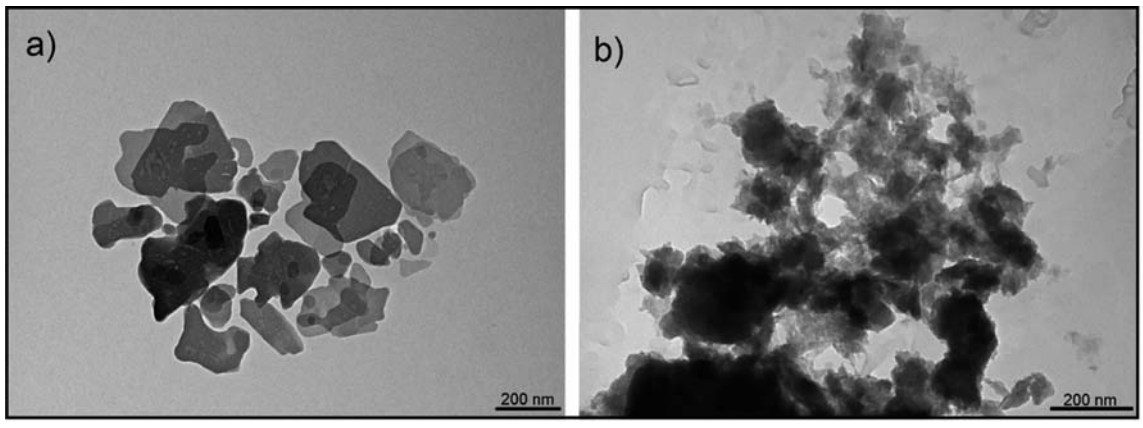

Figure 5. TEM images of the pristine α-ZrP particles (a) and $ZP(C_{10})_{1.01}$ (b) powder samples.

dx.doi.org/10.1021/ic400834d | Inorg. Chem. 2013, 52, 7680−7687

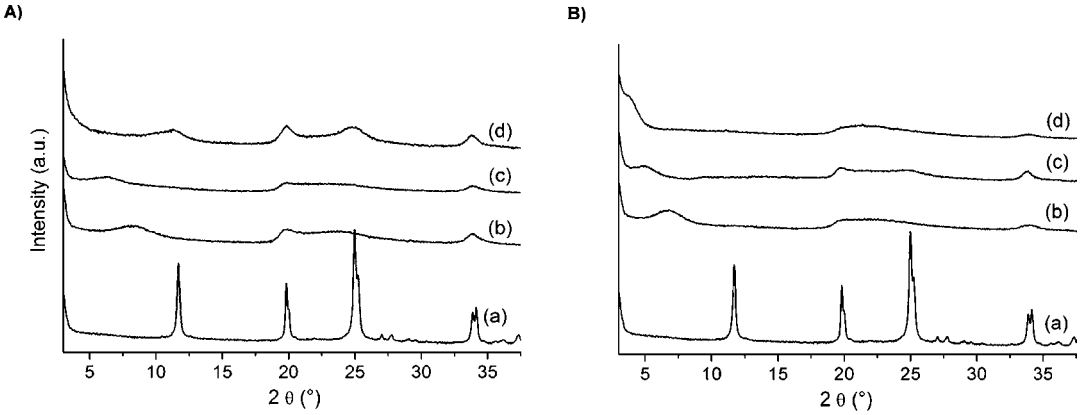

Figure 6. X-ray diffraction patterns of powder samples obtained for R = 0.4 (A) and R = 4.0 (B). (A): pristine α-ZrP (a); $ZP(C_4)_{0.19}$ (b); $ZP(C_6)_{0.30}$ (c); $ZP(C_{10})_{0.34}$ (d). (B): pristine α-ZrP (a); $ZP(C_4)_{1.14}$ (b); $ZP(C_6)_{0.87}$ (c); $ZP(C_{10})_{1.01}$ (d).

react with H_2C_n, the particle growth expected after solvent elimination is hindered to some extent by the presence of the C_n groups.

3.1.4. X-ray Diffraction Analysis. α-type ZrP is a well-known material consisting of layers made of zirconium atoms bridged, on both plane sides, by monohydrogen phosphate groups.[19] Three oxygens of each phosphate group are bonded to three different Zr atoms, and each Zr atom is octahedrally coordinated by six oxygens. The fourth oxygen of the phosphate group bonds to a proton and points into the interlayer space. The water molecules sit in the interlayer region, forming a hydrogen-bonding network with the phosphate groups. The distance between the barycenters of two adjacent layers, called interlayer distance, is 7.56 Å.

The X-ray diffraction pattern of the pristine ZrP is compared in Figure 6 with the patterns of the $ZP(C_n)_x$ powder samples, obtained for R = 0.4 and R = 4.0 and dried at 120 °C.

In general, the patterns of the dried samples differ to a large extent from the pattern of pristine α-ZrP, except for the presence of the 020 reflection at 33.8° 2θ which remained unchanged in all cases. Recalling that this reflection is associated with the Zr−Zr separation in the α-type layer and that the ^{31}P NMR data indicate that the phosphonate groups have the same coordination as the monohydrogen phosphate groups, it is inferred that the replacement of alkylphosphonate groups for monohydrogen phosphate groups leaves unaltered the structure of the α-layer. Thus the reaction of α-ZrP with alkylphosphonic acids is a topotactic anion exchange reaction.

As regards the distribution of phosphonate groups in the α-type layer, it can be taken into account that for x < 2 different arrangements are possible, among which the following are two limit situations: (1) the reaction proceeds according to the "moving phase boundary" model where the phosphonate exchanged phase (with x up to 2) coexists with unreacted ZrP,[20] or (2) the phosphonate groups are randomly distributed among the monohydrogen phosphate groups. Correspondingly, the X-ray patterns should show (1) the 002 reflection of the exchanged phase along with that of the unreacted phase or (2) a continuous shift of the 002 reflection of the pristine material toward low θ values as the reaction proceeds. This was actually observed at increasing x values for the patterns of the gel materials. We therefore conclude that the topotactic exchange reaction leads to the formation of single-phase mixed compounds where the alkylphosphonate groups are grafted onto the α-layers, being randomly distributed among unreacted monohydrogen phosphate groups. In agreement with this arrangement, the interlayer distances obtained for $ZP(C_4)_{1.07}$, 13.2 Å, and $ZP(C_6)_{0.80}$, 15.0 Å, (Figure 7A and 7B, patterns b) lie between those of the pure alkylphosphonates (d = 15.9 Å for $Zr(C_4)_2$, d = 19.2 Å for $Zr(C_6)_2$)[21] and phosphate phases.[22]

It is also known that a random arrangement, within the interlayer region, of large organic groups and small hydroxyl groups, results in cavities, in which solvent molecules can be accommodated.[7f,21,23] In this regard, it is interesting to compare the X-ray patterns of the gels with those of the corresponding materials obtained by heating the gels at 120 °C (Figure 7). It can be observed that the 002 reflection of $ZP(C_4)_{1.07}$ and $ZP(C_6)_{0.80}$ shifts after drying to slightly higher 2θ values, getting broader and less intense.

Correspondingly the interlayer distances decrease from d = 15.8 to 13.2 Å for $ZP(C_4)_{1.07}$ and from d = 17.6 Å to 15.0 Å for $ZP(C_6)_{0.80}$. A similar behavior is observed for $ZP(C_{10})_{0.96}$ but, in this case, the broadening and the decrease in intensity of the 002 reflection are too strong to allow an accurate estimation of the interlayer distance. The evolution of the X-ray patterns of the gels upon heating suggests the presence of free volume among the alkyl chains, which is likely to be filled by propanol in the gel material and which collapses when the gel is dried. These findings are consistent with previous works[23,7f,11a] showing that the random arrangement of two groups with different size in the interlayer space promote the formation of highly irregular structures with "porous pathways".

The formation of single-phase mixed compounds represents a novelty with respect to that found by Hix et al.[13] In that case, the topotactic exchange replacement of monohydrogen phosphate groups with phenylphosphonate groups on semi-crystalline α-ZrP led to mixtures of pure phases of α-ZrP and α-zirconium phenylphosphonate with constant composition.

3.2. Polymer Composite. One of the most fascinating aspects of this work was the possibility to prepare gels of zirconium alkylphosphonate nanoplatelets which are particularly suitable as fillers in the preparation of polymer nanocomposites. As a matter of fact, the presence of accessible space among the alkyl chains is expected to promote the filler−polymer interaction leading eventually to the filler exfoliation.

On the basis of the above considerations, a gel of $ZP(C_6)_{0.54}$ was used to prepare a potato starch composite membrane. Starch consists of one branched (amylopectin) and one linear (amylose) polymer made of D-glucose units. The idea was to disperse, within starch, an inorganic filler which could act as

dx.doi.org/10.1021/ic400834d | Inorg. Chem. 2013, 52, 7680−7687

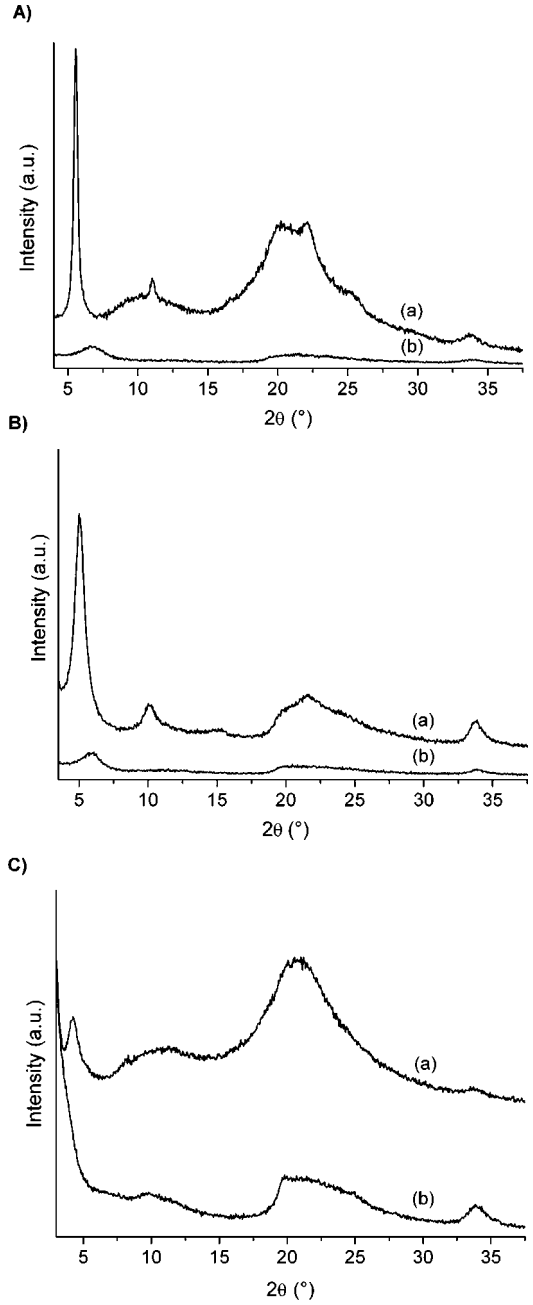

Figure 7. X-ray diffraction patterns of $ZP(C_4)_{1.07}$ (A), $ZP(C_6)_{0.80}$ (B), $ZP(C_{10})_{0.96}$ (C). Patterns (a) refer to gels, patterns (b) refer to powder samples obtained by drying the corresponding gels at 120 °C for 15 h.

mechanical reinforcement and, at the same time, as plasticizer for the polymer matrix to obtain plastic materials, based on a biodegradable polymer, mechanically stronger than the traditional glycerol-based starch films.[24,25] With this aim, propanol in the $ZP(C_6)_{0.54}$ gel was first replaced by water and then the aqueous gel was mixed to gelatinized starch in water. A transparent and very flexible film was obtained after casting and solvent evaporation (Figure 8). This is a remarkable result, especially if one considers that attempts to prepare starch membranes filled with naked α-ZrP particles were unsuccessful since they turned out to be highly brittle and hard to handle.

3.2.1. Structural and Morphological Characterization. The SEM images of the starch/$ZP(C_6)_{0.54}$ membrane are reported in Figure 9. The image collected with secondary electrons

Figure 8. Picture of a starch membrane containing 5 wt % $ZP(C_6)_{0.54}$.

(Figure 9a) shows a dense and homogeneous matrix where the filler particles cannot be distinguished from the polymer at the micrometer scale. This is confirmed by the image collected with backscattered electrons (Figure 9b), which shows, in addition, the presence of diffuse light gray domains, where the filler is probably more concentrated.

The X-ray diffraction pattern of the starch composite film is reported in Figure 10(d), together with that of the native starch (a), a film obtained by gelatinizing starch in hot water (b), a glycerol-plasticized starch film (c), a physical mixture of starch and 5 wt % $ZP(C_6)_{0.54}$ powder samples (e).

As far as starch is concerned, the broadening and the intensity decrease of the main starch reflections[26] reveals a significant disruption of the semicrystalline structure of the native starch granules (pattern a) as a consequence of the thermal treatment in water (pattern b) and the presence of glycerol (pattern c). The pattern of the composite much resembles those of water-gelatinized and glycerol-based starch films, indicating that a substantially amorphous network is present also in that system. Moreover, no distinct peaks ascribable to the filler are observed in the pattern of the composite film (d); in particular, while the pattern of the starch/$ZP(C_6)_{0.54}$ physical mixture (e) shows the presence of the reflection at 33.8° 2θ, typical of the α-layer structure of zirconium phosphates and phosphonates, this peak is missing in the pattern of the composite film, suggesting that the filler particles are randomly distributed within the polymer matrix.

3.2.2. Mechanical Properties. Figure 11 displays the stress−strain curve of the starch/$ZP(C_6)_{0.54}$ membrane, compared with that of a reference glycerol-starch membrane.

The presence of the filler significantly increases the slope of the curve in the elastic region, as well as the yield stress, indicating that the composite film is mechanically stronger than the reference film. For example, the modulus of resilience of the composite, that is, the maximum energy that can be absorbed per unit volume without creating a permanent distortion (estimated from the area of the stress−strain curve from zero to the elastic limit) is about three times higher than that of the glycerol-starch film. This improvement is associated to a decrease in the elongation at the break point because of a reduction of the plastic deformation. It is however noteworthy that the composite film exhibits good flexibility.

As expected from the stress−strain curves, the Young's modulus increased significantly, going from 734 (±45) MPa to

dx.doi.org/10.1021/ic400834d | Inorg. Chem. 2013, 52, 7680−7687

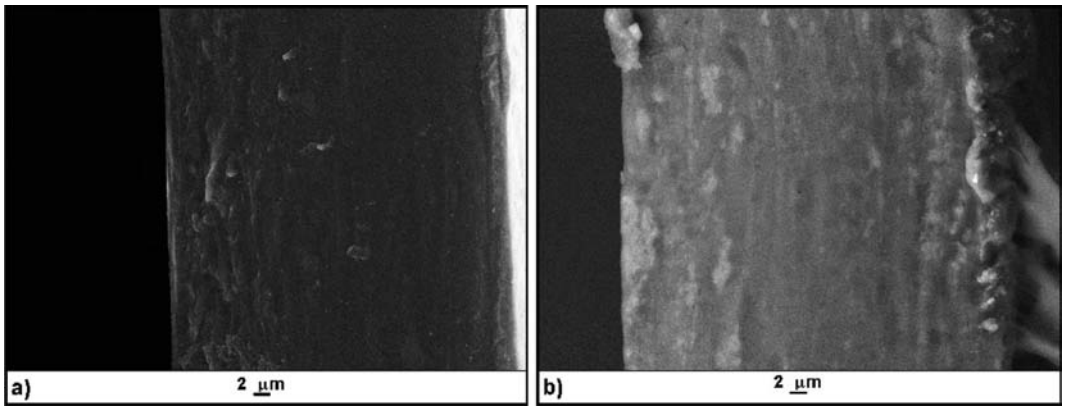

Figure 9. SEM images of a starch/ZP$(C_6)_{0.54}$ membrane collected with secondary (a) and backscattered (b) electrons.

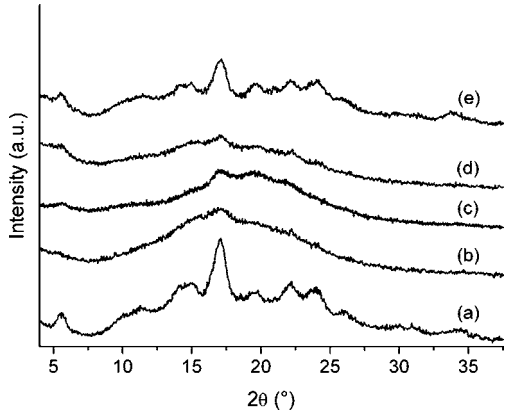

Figure 10. X-ray diffraction patterns of native starch (a); a film obtained by gelatinizing starch in hot water (b); a glycerol-plasticized starch film (c); a starch/ZP$(C_6)_{0.54}$ composite membrane (d); a physical mixture of starch and 5 wt % ZP$(C_6)_{0.54}$ powder samples (e).

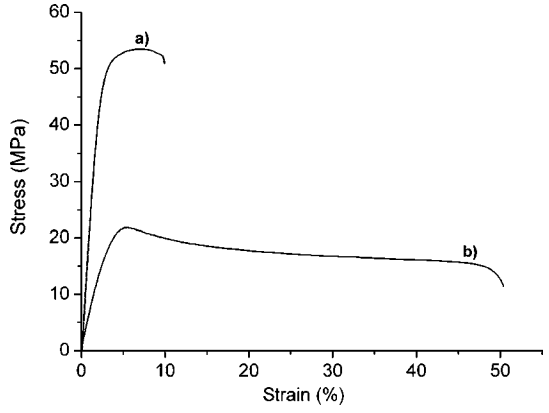

Figure 11. Stress–strain curves of a starch/ZP$(C_6)_{0.54}$ membrane (a), and a glycerol-starch membrane (b).

2423 (±145) MPa (230% proportional increase), while the yield stress passed from 17.4 (±2.4) MPa to 53.3 (±6.9) MPa (206% proportional increase). Although this is only a preliminary study, this result is undoubtedly promising and deserves the right attention.

4. CONCLUSIONS

For the first time, nanosized layered α- zirconium(IV) alkylphosphonates were prepared by a topotactic anion exchange reaction, at room temperature, employing propanol intercalated α-ZrP nanoparticles and solutions of alkylphosphonic acids in propanol. ^{31}P MAS NMR, together with X-ray analysis, proved that a topotactic anion exchange reaction effectively occurred, leading to a random distribution of the alkylphosphonate groups on the α-type layers. The resulting accessible volume among the alkyl chains is expected to promote the dispersion of the ZP$(C_n)_x$ nanoparticles within a polymer matrix. Accordingly, ZP$(C_6)_{0.54}$ was employed as filler for potato starch. A preliminary starch membrane filled with 5 wt % ZP$(C_6)_{0.54}$ exhibited excellent mechanical properties combining high Young's modulus (about three times higher than that of a traditional glycerol/starch membrane) with high flexibility and handleability.

The present approach turned out to be a quick and efficient method to prepare inorgano-organic layered Zr(IV) compounds. Ideally, almost any organic molecule can be converted into a phosphonic acid derivative, so as to generate infinite combinations for layered metal phosphonates. Besides the fact that the functionalization with phosphonate groups can be easily studied by ^{31}P MAS NMR, the proposed method allows to effectively control the composition of the zirconium phosphonates and, consequently, to modulate their properties, without significantly affecting the morphology of the precursor ZrP nanoparticles. In conclusion, the present strategy blazes new trails in the field of polymer composites, since it offers the possibility to obtain tailor-made inorgano-organic nanofillers, which can be easily dispersed within a polymer dispersion or a melt.

AUTHOR INFORMATION

Corresponding Author

*E-mail: monica.pica@unipg.it. Phone: +39 075 585 5564. Fax: +39 075 585 5566.

Notes

The authors declare no competing financial interest.

ACKNOWLEDGMENTS

The authors wish to thank Dr. Alessandro Di Michele of the LUNA Laboratory, at the Physics Department of Perugia University, for collecting SEM pictures and Professor Riccardo Vivani for the realization of the Table of Contents picture.

REFERENCES

(1) Neouze, M.-A.; Schubert, U. *Monatsh. Chem.* **2008**, *139*, 183–195.

(2) Queffélec, C.; Petit, M.; Janvier, P.; Knight, D. A.; Bujoli, B. *Chem. Rev.* **2012**, *112*, 3777−3807.
(3) Díaz, A.; Mosby, B. M.; Bakhmutov, V. I.; Martí, A. A.; Batteas, J. D.; Clearfield, A. *Chem. Mater.* **2013**, *25*, 723−728.
(4) (a) Cao, G.; Ong, H. U.-G.; Mallouk, T. E. *Acc. Chem. Res.* **1992**, *25*, 420−427. (b) Thompson, M. E. *Chem. Mater.* **1994**, *6*, 1168−1175. (c) Alberti, G.; Casciola, M.; Costantino, U.; Vivani, R. *Adv. Mater.* **1996**, *8*, 291−303. (d) Clearfield, A. *Curr. Opin. Solid State Mater. Sci.* **1996**, *1*, 268−278. (e) Alberti, G.; Casciola, M. *Solid State Ionics* **1997**, *97*, 177−186. (f) Mutin, P. H.; Guerrero, G.; Vioux, A. *C. R. Chim.* **2003**, *6*, 1153−1164. (g) Vivani, R.; Alberti, G.; Costantino, F.; Nocchetti, M. *Microporous Mesoporous Mater.* **2008**, *107*, 58−70. (h) Brunet, E.; Alhendawi, H. M H.; Alonso, M.; Cerro, C.; Jiménez, L.; Juanes, O.; Mata, M. J.; Salvador, , A.; Victoria, M.; Rodríguez-Payán, E.; Rodríguez-Ubis, J. C. *J. Phys.: Conf. Ser.* **2010**, *232*, 1−8. (i) Taddei, M.; Costantino, F.; Manuali, V.; Vivani, R. *Inorg. Chem.* **2011**, *50*, 10835−10843. (j) *Metal Phosphonate Chemistry: From Synthesis to Applications*; Clearfield, A., Demadis, K. D., Eds.; RSC Publishing: Cambridge, U.K., 2011.
(5) Alberti, G.; Costantino, U.; Allulli, S.; Tomassini, N. *J. Inorg. Nucl. Chem.* **1978**, *40*, 1113.
(6) (a) Alberti, G.; Casciola, M.; Costantino, U.; Peraio, A.; Montoneri, E. *Solid State Ionics* **1992**, *50*, 315−322. (b) Alberti, G.; Casciola, M.; Palombari, R.; Peraio, A. *Solid State Ionics* **1992**, *58*, 339−344. (c) Alberti, G.; Boccali, L.; Casciola, M.; Massinelli, L.; Montoneri, E. *Solid State Ionics* **1996**, *84*, 97−10.
(7) (a) Alberti, G.; Casciola, M.; Pica, M.; Di Cesare, G. *Ann. N.Y. Acad. Sci.* **2003**, *984*, 208−225. (b) Alberti, G.; Casciola, M.; D'Alessandro, E.; Pica, M. *J. Mater. Chem.* **2004**, *14*, 1910−1914T. (c) Alberti, G.; Casciola, M.; Pica, M.; Tarpanelli, T.; Sganappa, M. *Fuel Cells* **2005**, *5*, 366−374. (d) Casciola, M.; Capitani, D.; Donnadio, A.; Diosono, V.; Piaggio, P.; Pica, M. *J. Mater. Chem.* **2008**, *18*, 4291−4296. (e) Casciola, M.; Capitani, D.; Donnadio, A.; Frittella, V.; Pica, M.; Sganappa, M. *Fuel Cells* **2009**, *4*, 381−386. (f) Sun, L.; Liu, J.; Kirumakki, S. R.; Schwerdtfeger, E. D.; Howell, R. J.; Al-Bahily, K.; Miller, S. A.; Clearfield, A.; Suef, H.-J. *Chem. Mater.* **2009**, *21*, 1154−1161. (g) Donnadio, A.; Pica, M.; Taddei, M.; Vivani, R. *J. Mater. Chem.* **2012**, *22*, 5098.
(8) Youngblood, W. J.; Lee, S.-H. A.; Maeda, K.; Mallouk, T. E. *Acc. Chem. Res.* **2009**, *42*, 1966−1973.
(9) Monot, J.; Petit, M.; Lane, S. M.; Guisle, I.; Léger, J.; Tellier, C.; Talham, D. R.; Bujoli, B. *J. Am. Chem. Soc.* **2008**, *130*, 6243−6251.
(10) (a) Colón, J. L.; Thakur, D. S.; Yang, C.-Y.; Clearfield, A.; Martini, C. R. *J. Catal.* **1990**, *124*, 148−159. (b) Curini, M.; Rosati, O.; Costantino, U. *Curr. Org. Chem.* **2004**, *8*, 591−606. (c) Bellezza, F.; Cipiciani, A.; Costantino, U.; Nicolis, S. *Langmuir* **2004**, *20*, 5019−5025. (d) Ma, X.; Wang, Y.; Wang, W.; Cao, J. *Catal. Commun.* **2010**, *11*, 401−407. (e) Chen, T.; Ma, X.; Wang, X.; Wang, Q.; Zhou, J.; Tang, QJ. *Dalton Trans.* **2011**, *40*, 3325.
(11) (a) Wang, J. D.; Clearfield, A.; Guang-Zhi, P. *Mater. Chem. Phys.* **1993**, *35*, 208−216. (b) Rosenthal, G. L.; Caruso, J. *J. Solid State Chem.* **1993**, *107*, 497−502. (c) Alberti, G.; Casciola, M.; Donnadio, A.; Piaggio, P.; Pica, M.; Sisani, M. *Solid State Ionics* **2005**, *176*, 2893−2898. (d) Amicangelo, J. C.; Leenstra, W. R. *Inorg. Chem.* **2005**, *44*, 2067−2073.
(12) (a) Yamanaka, S.; Sakamoto, K.; Hattori, M. *J. Phys. Chem.* **1984**, *88*, 2067−2070. (b) Alberti, G.; Casciola, M.; Vivani, R.; Biswas, R. K. *Inorg. Chem.* **1993**, *32*, 4600−4604. (c) Alberti, G.; Giontella, E.; Mascaros, S. M. *Inorg. Chem.* **1997**, *36*, 2844−2849. (d) Brunet, E.; Alhendawi, H. M.H.; Cerro, C.; de la Mata, M. J.; Juanes, O.; Rodríguez-Ubis, J. C. *Microporous Mesoporous Mater.* **2011**, *138*, 75−85.
(13) Hix, G. B.; Kitchin, S. J.; Harris, K. D. M. *J. Chem. Soc., Dalton Trans.* **1998**, 2315−2319.
(14) Pica, M.; Donnadio, A.; Capitani, D.; Vivani, R.; Troni, E.; Casciola, M. *Inorg. Chem.* **2011**, *50*, 11623−11630.
(15) Massiot, D.; Fayon, F.; Capron, M.; King, I.; LeCalvé, S.; Alonso, B.; Durand, J. O.; Bujoli, B.; Gan, Z.; Hoatson, G. *Magn. Reson. Chem.* **2002**, *40*, 70−76.
(16) Clayden, N. *J. Chem. Soc., Dalton Trans.* **1987**, *8*, 1877.
(17) Casciola, M.; Capitani, D.; Comite, A.; Donnadio, A.; Frittella, V.; Pica, M.; Sganappa, M.; Varzi, A. *Fuel Cells* **2008**, *08*, 217−224.
(18) D'Andrea, S. C.; Fadeev, A. Y. *Langmuir* **2003**, *19*, 7904−7910.
(19) Clearfield, A.; Costantino, U. In *Comprehensive Supramolecular Chemistry*; Alberti, G., Bein, T., Eds.; Pergamon, Elsevier Science ltd Press: New York, 1996; Vol. *7*, Chapter 4.
(20) Alberti, G. *Acc. Chem. Res.* **1978**, *11*, 163−168.
(21) Alberti, G. In *Comprehensive Supramolecular Chemistry*; Alberti, G., Bein, T., Eds.; Pergamon, Elsevier Science ltd Press: New York, 1996; Vol. *7*, Chapter 5.
(22) Jaimez, E.; Bortun, A.; Hix, G. B.; García, J. R.; Rodríguez, J.; Slade, R. C. T. *J. Chem. Soc., Dalton Trans.* **1996**, 2285−2292.
(23) Boo, W. J.; Sun, L.; Liu, J.; Clearfield, A.; Sue, H.-J. *J. Phys. Chem. C* **2007**, *111*, 10377−10381.
(24) Janssen, L.; Moscicki, L., Eds.; *Thermoplastic Starch*; Wiley-VCH: Weinheim, Germany, 2009.
(25) Talja, R. A.; Helen, H.; Roos, Y. H.; Jouppila, K. *Carbohydr. Polym.* **2007**, *67*, 288−295.
(26) Cheetham, N. W. H.; Tao, L. *Carbohydr. Polym.* **1998**, *36*, 277−284.